16

Functional and Structural Evaluation of Retrobulbar Glaucomateus Damage

Kaya N Engin
Bagcilar Education and Research Hospital,
Department of Ophthalmology Istanbul
Turkey

1. Introduction

Glaucoma represents a group of neurodegenerative diseases characterized by structural damage to the optic nerve and the slow, progressive death of retinal ganglion cells (RGCs). Elevated intraocular pressure (IOP) is traditionally considered to be the most important risk factor for glaucoma, and treatment options for the disease have hitherto been limited to its reduction. However, visual field loss and RGC death continue to occur in patients with well controlled IOPs (Chidlow et al, 2007). Currently, increased IOP has been excluded from the definition of glaucoma, considered a major risk factor, and glaucoma has been defined as an optic neuropathy. Though we have effective medical and surgical therapies at hand, progressive visual loss is still a prevalent symptom in glaucoma cases. Evidence today proves that glaucomatous damage proceeds from RGCs to the brain (Weinreb, 2007).

The ophthalmologist is fully aware that he/she is dealing with the whole visual system –not just the globe, in many neuro-ophthalmic disorders, knowing a defect in the visual field can be due to much pathology from the globe to cortex. Today, we should take areas beyond the retina and optic nerve into consideration in glaucoma follow ups as well. If we recall the anatomy, it is as follows: the retina, optic nerves, optic chiasm, optic tracts, lateral geniculate nuclei (LGN), other brainstem primary visual nuclei (superior colliculus, pretectum), hypothalamic nuclei, pulvinar and accessory optic system, geniculostriate (optic) radiations, striate cortex, visual association areas, and related interhemispheric connections constitute the primary visual sensory system in humans. The optic nerve consists of four segments: intraocular (1 mm in length), intraorbital (about 25 to 30 mm), intracanalicular (about 9 to 10 mm), and intracranial (about 16 mm). Thus, the entire length of the optic nerve from the globe to the optic chiasm is about 5 to 6 cm.

Behind the laminar cribrosa, the optic nerve abruptly increases in diameter from 3 mm to 4 mm in midorbit and to 5 mm intracranially. The optic chiasm derives from the merging of the two optic nerves and sits 10.7 ± 2.4 mm above the dorsum of the sella turcica. Occasionally, the intracranial optic nerves are shorter, and the chiasm may lie directly above the sella in a position that is called "prefixed." More commonly, the optic chiasm is positioned 10 to 12 mm above the insertion of the diaphragma sellae onto the dorsum. The significance of this region arises from the fact that lateral fibers originating from the temporal side of the globe directly pass it, while medial fibers originating from the nasal side cross over to the opposite hemisphere (Figure 1). As the retinofugal fibers pass through

the chiasm, they form the optic tracts immediately posterior to the optic chiasm. Each tract begins at the posterior notch of the chiasm and is separated from the other optic tract by the pituitary stalk inferiorly and the third ventricle more superiorly. Most of the fibers in the optic tract terminate in the ipsilateral LGN. With the accessory fibers from other nuclei they form the optic radiation (geniculocalcarine fiber tract) and constitute the "posterior" visual pathway that projects to the primary visual cortex. The primary visual cortex goes by many names, such as striate cortex, area 17, or as used in experimental research, V1. These visual fibers then turn medially above and below the occipital horn to terminate in the mesial surface of the occipital lobe, the striate (calcarine) cortex. The visual cortex extends anteriorly toward the splenium of the corpus callosum and is separated into a superior and an inferior portion by the calcarine fissure, which runs horizontally (Sadun, 2007).

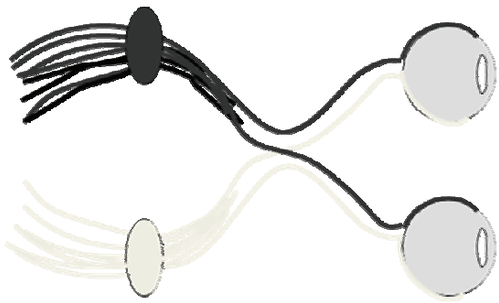

Fig. 1. Cross-over of nasal and temporal fibers in optic chiasm.

2. Glaucoma as a brain disease

2.1 Histopathological studies

Gupta and Yücel have provided primary evidence that glaucomatous damage extends from RGCs to vision centers in the brain. They have observed degenerative and/or neurochemical changes in the LGN, magno-, parvo-, and koniocellular pathways, and changes in metabolic activity in both the LGN and visual cortex in glaucoma (Gupta & Yücel, 2003). The same group elicited many subsequent studies in this area thereafter. In an experimental primate model of unilateral glaucoma, they observed degenerative changes in magnocellular, parvocellular, and koniocellular pathways in the LGN, and these changes are presented in relation to IOP and the severity of optic nerve damage. Neuropathological findings were also present in LGN layers driven by the unaffected fellow eye. Finally, there was information on changes in the visual cortex in relation to varying degrees of RGC loss (Yucel et al, 2003).

The first clinicopathological case of human glaucoma, demonstrating degenerative changes in the brain involving the intracranial optic nerves, LGN, and visual cortex have been reported by the same group. Postmortem specimens of a 79 year old, healthy white male - with a large cup to disc ratio of 0.9, deep excavation and loss of the inferotemporal rim, was compared with 4 controls in the same age group. Optic nerve atrophy in glaucoma compared to control optic nerves was pronounced. Marked axonal loss was also evident inferiorly in the right and left glaucoma optic nerves. Compared to the control, there was striking overall LGN shrinkage in glaucoma. Nissl stained sections showed magnocellular parvocellular neurons with smaller, more globoid cytoplasm and smaller nucleus in glaucoma compared to stellate neurons seen in the controls. Lipofuscin pigment deposits occupied more of the cytoplasm in glaucoma compared to the controls. In the visual cortex

representing the visual field defect, cortical ribbon thickness reduction was easily discernible compared to the controls (Gupta et al, 2006).
They also put forward that numerous similarities exist between glaucoma and neurodegenerative diseases, such as Alzheimer's and Parkinson's disease. Similarities include the selective loss of neuron populations, transsynaptic degeneration in which disease spreads from injured neurons to connected neurons, and common mechanisms of cell injury and death. Mechanisms involved in central visual system damage in glaucoma included oxidative injury and glutamate toxicity, as seen in neurodegenerative diseases. Similar to many neurodegenerative diseases, those changes have been histopathologically proven to be prevented by the use of Memantine (Gupta & Yücel, 2007).
In the light of these studies, the importance of IOP-independent strategies in the treatment of glaucoma increases, while studies for in vivo demonstration of brain damage in patients with glaucoma accelerate. For this purpose, the most commonly used technology is magnetic resonance imaging (MRI).
The first key findings have been obtained with Functional MRI (fMRI). Increases in neuronal activity are accompanied by changes in blood oxygenation that give rise to changes in the MR signal. First, local concentrations of deoxyhemoglobin generate magnetic field gradients along the blood vessels reduce the MR signal. Second, increases in neuronal activity result in decreases in the local oxygen extraction fraction in the blood that, in turn, causes a corresponding drop in the local concentration of deoxyhemoglobin. The net reduction of deoxyhemoglobin during brain activity manifests in an increase in MR signal known as blood oxygenation level dependent (BOLD) signals. Mapping BOLD signals is called "Retinotopic Organisation" (Duncan et al, 2007).
Another important MRI technique for imaging visual pathways is Diffusion-Tensor MRI (DTI). It is based on the movement principle of fluids in a plane connected to the nerve. Water diffusion in biological tissues, such as white matter occurs preferentially parallel to the orientation of axons. Such diffusion is known as anisotropic diffusion which depends on the structural environment of white matter. DTI provides a complete description of water diffusion in three dimensions. Radial (λ1) and axial diffusivities (λ2, λ3) form anisotropy and it is estimated as fractional anisotropy (FA). Axial diffusivities can be expressed as a single value, λ//. A nerve can be traced with anisotropy maps, a process referred to as "Tractography" (Nucifora et al, 2007) (Figure 2).

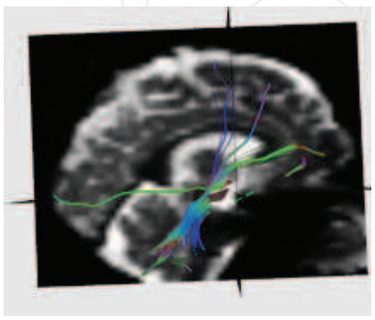

Fig. 2. Imaging nerve fibers with "Tractography" method.

2.2 Animal studies

Retrobulbar neuro-degeneration could be demonstrated in experimental glaucoma models with different MRI techniques. In a rat model of chronic glaucoma, choline reduction in the

visual cortex was revealed with proton magnetic resonance spectroscopy. Relative to the creatine level, the choline level was found to be significantly lower in the left glaucomatous visual cortex than the right control visual cortex in all animals. In addition, a marginally significant increase in the glutamate level was observed in the glaucomatous visual cortex. Authors concluded that, measurement of the Cho:Cr reduction in the visual cortex may be a noninvasive biomarker for this disease (Chan et al, 2009).

In a DTI study with 7T MRI, experimental glaucoma was performed on seven rats by substantial photocoagulation of the episcleral and limbal veins of the right eyes with Argon laser, whereas the left eye served as the control. It was shown for the first time that *in vivo* DTI can be successfully applied to detect axonal density changes occurring in the rat model of glaucoma. As much as 10% decrease in axonal density of the glaucomatous ON was detected in enlarged B_0 coronal plane images by an approximately 30% increase in $\lambda 1$ and 5% decrease in FA with no significant change in that of $\lambda //$. In the same study, those findings are also histopathologically confirmed (Hui et al, 2007).

2.3 Retrobulber imaging in humans

The optical nerve is of specific importance since it is among structures heavily influenced by glaucomatous neuro-degeneration and it provides information on the ipsilateral eye. In a study conducted with conventional MRI in patients with glaucoma, it was reported that the diameter of the optic nerve was significantly lower, and that the optic chiasm was shorter in comparison with that of the controls and those findings correlated with deterioration in MD values rather than c/d ratios (Kashiwagi et al, 2004).

In a more recent study, as a biomarker for axonal loss in glaucomatous optic atrophy, the retrobulbar optic nerve was diameter measured by ultrafast high-resolution MRI at 3T. Included in the study was one eye each from 47 subjects, of whom 9 had no eye disease, 16 had preperimetric glaucoma, 11 had a glaucomatous mean visual field defect of <10 dB and 11 of >10 dB. OND was found to be correlated best with the retinal nerve fiber layer thickness measured by an optic coherence tomography (Lagrèze et al, 2009).

Another study was conducted in 26 patients with primary open-angle glaucoma (POAG), and 26 control subjects. In the patient group, the presence of white matter hyperintensities (WMH) was evaluated more on fluid-attenuated inversion recovery images of the brain. Both the area of the optic nerves and the magnetisation transfer ratio (MTR) measured in the chiasm and in the grey and white matter of the calcarine fissure were lower. Authors used Conventional MRI and magnetisation transfer imaging of the brain and optic pathway and concluded that, POAG leads to optic nerve atrophy and degeneration of the optic pathway. The finding of the increase in the number of WMH implies that cerebrovascular disease may play a role in the pathogenesis of POAG (Kitsos et al, 2009).

One of most important techniques in the structural evaluation of nervous tissue is DTI. The optical tract in humans could be imaged from CGL to calcarine sulcus using this method (Sherbondy et al, 2008). Garaci et al. examined glaucomatous damage in humans over 16 patients with POAG and 10 control subjects. Sixteen patients with POAG were examined. Glaucoma severity was clinically assessed with the use of a six-stage system based on static threshold visual field parameters. DTI was performed with a 3-T MR unit. Mean diffusivity (MD) and fractional anisotropy (FA) maps were automatically created. Regions of interest were positioned in three spots for each evaluation. They found that, the optic radiations and optic nerves of patients with glaucoma, compared to the control subjects, had significantly

higher MD and significantly lower FA. A negative correlation between the mean FA for the optic nerves and glaucoma stage was reported (Garaci et al, 2009). Optic radiations were evaluated in another DTI study conducted with a 3T high-field magnetic resonance scanner in 50 glaucoma patients and 50 healthy age-matched controls in which anterograde and retrograde transneuronal rarefaction of the optic radiation were reported (Engelhorn et al, 2011)
The study emphasizing the importance of functionally examining the optical pathways in terms of glaucoma was conducted by Duncan et al. This study, which was first to in vivo confirm of interconnection between glaucoma and the brain, also used the 3T MRI and fMRI technique. Six asymmetric POAG patients with one glaucomatous eye and a less affected ''fellow'' eye were included. Patients' fellow eyes had markedly fewer visual field abnormalities relative to the glaucomatous eye. A long and complicated stimulus was given to the patients in three sessions to produce neuronal activity. The template fitting technique was used to project patterns of visual field loss onto the cortex. A comparison was made between the BOLD responses to the scotoma-mapping stimulus and the PSD from visual field testing for each patient yielding PSDDIF scores. A ''pointwise'' comparison of thresholds throughout the visual field to fMRI responses in corresponding locations of V1 was also conducted. They demonstrated that the pattern of VF loss observed using SAP is reflected by the pattern of BOLD activity in V1, and fMRI responses correlate with visual function thresholds (Duncan et al, 2007).
With a similar methodology, decreased cortical activity in the primary visual cortex of cases with POAG have been reported once again. The resultant cortical depression is stated to be unrelated to interocular differences in results of polarimetry, OCT, and ophthalmoscopy, but is negatively correlated with PSD of visual field analysis (Qing et al, 2010).
Imaging of CGL constitutes a great challenge. Arterial Spin Labeling fMRI -which provides direct measures of functional cerebral blood flow (CBF) changes, was used by Lu et al. in five healthy subjects. In this study, the baseline CBF in each LGN was estimated by averaging the signal measured during the off period (e.g. lack of hemispheric stimulus) for that LGN (Lu et al, 2008).
The Occipital Proton MR Spectroscopy technique, which detects low levels of N-Acetylaspartate in cortex areas receiving poor stimulation, was tried in patients with glaucoma and age-dependent macula degeneration. However, on the contrary to the above mentioned animal study, a reduction in metabolite levels in areas matching the progressive visual field in those patients could not be observed (Boucard et al, 2007).

3. Clinical evaluation of glaucomatous neuro-degeneration

3.1 Introduction

Above, we mentioned the possibilities provided by recent medicine via retrobulbar glaucomatous damage and the compatibility of resultant structural and functional findings with each other and histopathological and animal studies. In recent practice, we most frequently use Optical Coherence Tomography (OCT) and Visual Fields (VF), in decreasing order, in order to structurally and functionally examine glaucomatous damage in the eye. We have current knowledge regarding either advantages and disadvanteges of these two techniques or congruity of the data obtained. Although VF have been known to be a subjective method in glaucoma follow-ups, studies in large series revealed that OCT also possesses its own individual variability. Three factors that contribute to Retinal Nerve Fiber Layer (RNFL) variability in this range were identified. First, diseases of the inner retina can contribute to

artifactual thickening in some patients. Second, the individual variation in the visual field to disc mapping plays a role. Finally, the location of blood vessels, as well as the degree to which they are included by the RNFL algorithm, affects variability. Therefore, there is a considerable variability in the relationship between structure and function in glaucoma, even when care is taken to ensure that the data are of the highest quality (Hood et al, 2009). In addition, myopia (Rauscher et al, 2009) and the OCT technology used (Knight et al, 2009) are included in other variables. RNFL thickness, on the other hand, consists of two parts: RGC axons and nonaxon portion. Hood et al. assumes that the loss in the thickness of the axon portion is proportional to local field sensitivity loss, when field loss is expressed on a linear scale. That is, a 3-dB loss is associated, on average, with a loss of one half of the axon portion of the RNFL thickness, whereas the nonaxon portion is assumed to remain constant with RGC loss (Hood et al, 2007). However, the recently recognized approach is that glaucomatous damage affects both structure and function in linear proportion (Hood et al, 2009; Knight et al, 2009).
In our study, we examined the glaucoma – brain relation using a 1.5 T MRI device, which was in clinical use, and with DTI-MRI in terms of structure and with fMRI in terms of function; moreover, we examined those techniques with OCT and VF, respectively. In this manner, we aimed to non-invasively and comprehensively demonstrate eye – brain connection in glaucoma in humans, develop a method convenient for clinical use in order to use both in the diagnosis and follow-up of glaucoma and in studies with large case series, and finally to establish a strong reference for studies on the pathogenesis, follow-up and treatment of glaucoma.

3.2 Material and method

The eyes of an asymmetrical glaucoma patient and a healthy subject are included in this study. Care was taken that the control subject and patient did not have any known additional ocular, neurological or systemic diseases. Flow analysis was performed with color Doppler ultrasonography in the carotid, ophthalmic, posterior ciliar and central retinal arteries in order to eliminate ischemic pathology. While the central VF and MD and PSD values of the patient were recorded for functional analysis, retrobulbar assessment was performed with fMRI. Structural analyzes were completed by comparing c/d ratios with OCT and mean RNFL and ganglion cell (GCC) values with DTI. While the bilateral eyes of the patient were compared with each other and with the control, compatibility between structural and functional analyzes of globe and optic pathways was also evaluated.

DTI imaging

Imaging was performed with a 1.5 T Avanto Siemens (Erlangen, Germany) MRI device in Bakırköy Dr. Sadi Konuk Training and Research Hospital. Imaging protocol consisted of obtaining a high resolution T1 weighed (1x1x1mm) MPRAGE sequence, and fMRI time series images and diffusion weighed images, which are necessary for diffusion tensor imaging (DTI). For DTI, diffusion weighed images in 30 different directions and with 2 different b values (b=0,1000) were obtained. Imaging parameters were determined as TR=8200ms, TE=90ms, 2 mean, 3x3x3 isotropic voxel dimensions, a total of 60 slices and imaging duration of approximately 8 minutes. Diffusion weighed images were first separated from non-brain sections using FSL software. Using MedINRIA software on those images, diffusion tensor maps and fiber tractographs were created. Moreover, magnification was applied on b0 coronal plane images obtained from the same region and optic nerve morphologies were also evaluated on this plane (Figure 3).

DTI data analysis

A ROI (region on interest) 3 mm distance from the optic nerve was selected (Figure 4) and DTI parametric characteristic values (λ1, λ2, λ3) of the optic nerve were calculated. Using those measurements, FA and MD values were also estimated using formulas.

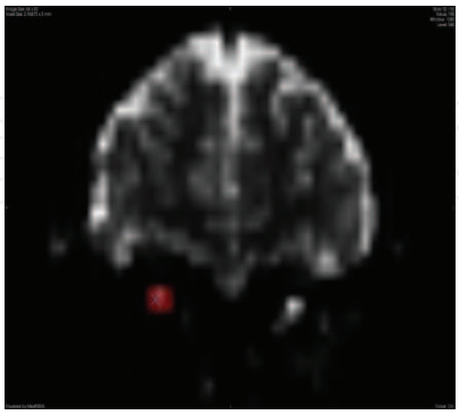

Fig. 3. Imaging optic nerve on b0 coronal plane images.

$$FA = \frac{\sqrt{3\left[(\lambda_1 - \langle\lambda\rangle)^2 + (\lambda_2 - \langle\lambda\rangle)^2 + (\lambda_3 - \langle\lambda\rangle)^2\right]}}{\sqrt{2(\lambda_1^2 + \lambda_2^2 + \lambda_3^2)}}, \langle\lambda\rangle = \frac{\lambda_1 + \lambda_2 + \lambda_3}{3}$$

Tracts have been drawn according to the ROIs, fiber count (SL), mean fiber length (d) and fiber volume (V) were recorded. Approximate slice areas were calculated with formula (A=V/d). Moreover, morphologies of the optic nerve were evaluated using b0 coronal plane images obtained from the same region.

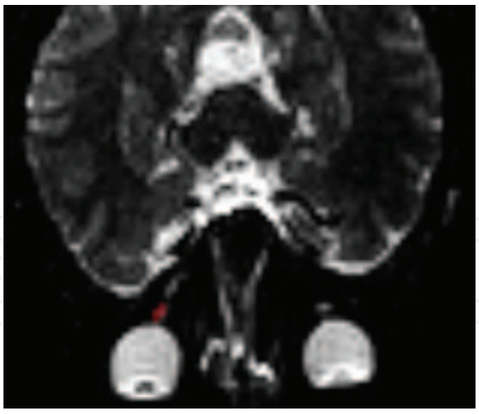

Fig. 4. ROI determination for diffusion analysis with DTI.

fMRI imaging

All fMRI imaging procedures were performed at Bakırköy Dr. Sadi Konuk Research Hospital using a 1.5 T Siemens MRI device. An anatomic image was obtained in 128 fractions in 1x1x1 cm resolution with a high resolution T1 weighed 3D GRE sequence. Functional MRI images were obtained with a GE-EPI sequence. In a 64x64 data collection matrix, 29 fractions covering visual cortex were obtained in resolutions of 3x3x3 mm voxel dimensions. TR was 2900ms, TE

30 was ms and the flip angle was 90 degrees. Sequential two imaging procedures were performed for the left and right eye of the patient with glaucoma. Thus, 544 volumes including 272 volumes for each eye were obtained from each individual.

Stimulation

Visual stimulation was prepared using OpenGL library and it was displayed by reflecting onto a mirror inside the MRI via an LCD projector and transparent curtain during the experiment. The visual field angle was measured as 40^0 on a horizontal plane and 25^0 on a vertical plane. The visual field was divided into five rings, each consisting of 12 sectors, and small spaces were left in order to differentiate each sector from the other. During the experiment, test subjects were asked to focus on the center point of the stimulation. Half of the selected 60 regions in the visual field along 67 blocks were flashed at a frequency of 8 Hz in the form of 4x4 chess boards. 68. No stimulation left in the block and the subject looked at blank screen.

fMRI data analyses

All functional analyzes were performed with SPM5 (by the Wellcome Department of Imaging Neuroscience, London, England). Following standard movement correction and fraction time correction procedures, all functional images were blurred using a Gausian spatial filter with FWHM of 5mm for modeling fMRI data, each of the 60 regions in the visual field were taken as a regressor and those regressors were used in the general linear model in SPM5. To model fMRI data, each regressor was convolved with standard hemodynamic response function.
For each of the 60 regions divided on the visual field, SPM(t) maps giving statistics of activation in relevant regions were created. Those maps were masked in the form of ($t > 3.12$, $p < 0.001$).
In order to compare activations occurring in the visual cortex, the visual field regions most heavily influenced by glaucoma were determined in each patient and activations occurring in the stimulation of those regions were calculated. For this purpose, voxel clusters exceeding the cut-off value in SPM(t) maps of each region were found and the percent change in BOLD was measured using fMRI corresponding to those clusters (Figure 5).

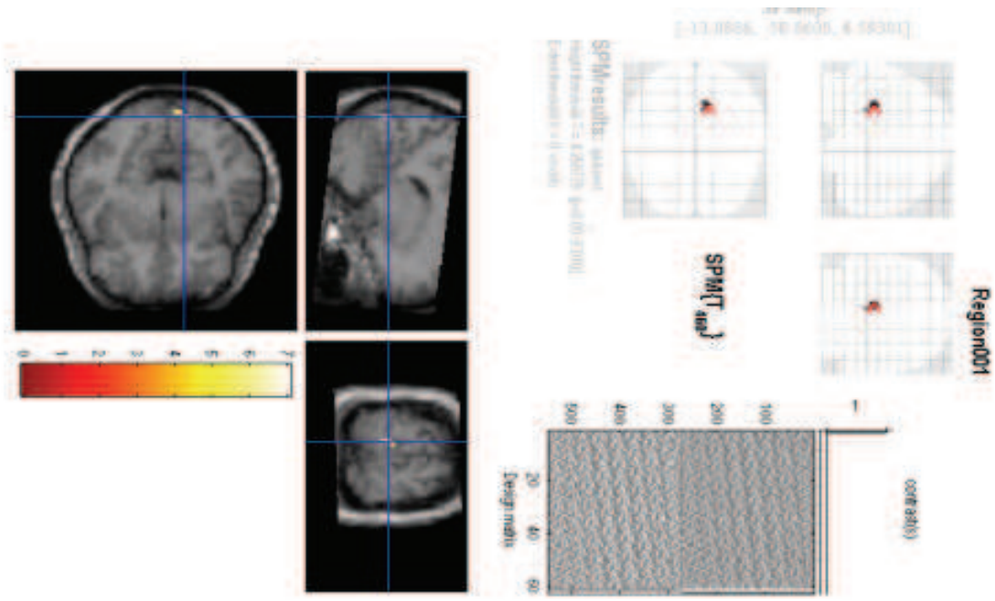

Fig. 5. Determination of BOLD signal in particular voxels

3.3 Results

In examinations performed with a Color Doppler ultrasonography, vascular anomaly was not observed in subjects. When the OCT findings of subjects (Table 1) were compared with the DTI diffusion analyzes (Table 2), reduction in all diffusion parameters in the eye with severe glaucoma relative to the other eye was observed for AC with asymmetrical involvement. In the comparison with the control, a reduction in MD and SL values was observed. High values in both mildly and severely glaucomatous eyes of AC were obtained relative to control.

		c/d	RNFL	GCC	PSD	MD
Control	Right	0.02	102.90	94,30	1,66	0,04
	Left	0	102.94	97,09	1,82	0,02
AC	Right	0,18	102,80	109,25	2,18	-2,75
	Left	0,45	71,04	82,16	11,13	-22,15

Table 1. OCT and VF findings of the control and the patient. RNFL: Retinal nerve fiber layer analysis, GCC: Ganglion cell counting, PSD: Pattern Standard Deviation, MD: Mean Deviation.

		FA	$\lambda 1$	$\lambda 2$	$\lambda 3$	MD	SL	V	d	A
Control	Right	0,17	3,21	2,63	2,08	2,64	4	185,083	20.05	9,23
	Left	0,15	3,41	2,96	2,57	2,98	4	158.64	20,78	7,63
AC	Right	0,37	2,54	1,69	1,19	1,806	4	350,967	13,50	26
	Left	0,325	2,08	1,43	1,07	1,526	2	134,987	12	11,25

Table 2. Diffusion analysis findings of the control and the patient. FA: Fractional anisotropy, $\lambda 1$: Radial diffusivity, $\lambda 2$, $\lambda 3$: Axial diffusivities, MD: Mean diffusivity, SL: Nerve fiber count, V: Volume, d: Maximum length, a: approximate cross-sectional area.

In b0 coronal plane images, when the control eyes (Figure 6A) and eyes with symmetrical involvement were compared, deterioration in the optic nerve diffusion of severely glaucomatous eyes of the patient with asymmetrical involvement was observed (Figure 6B)

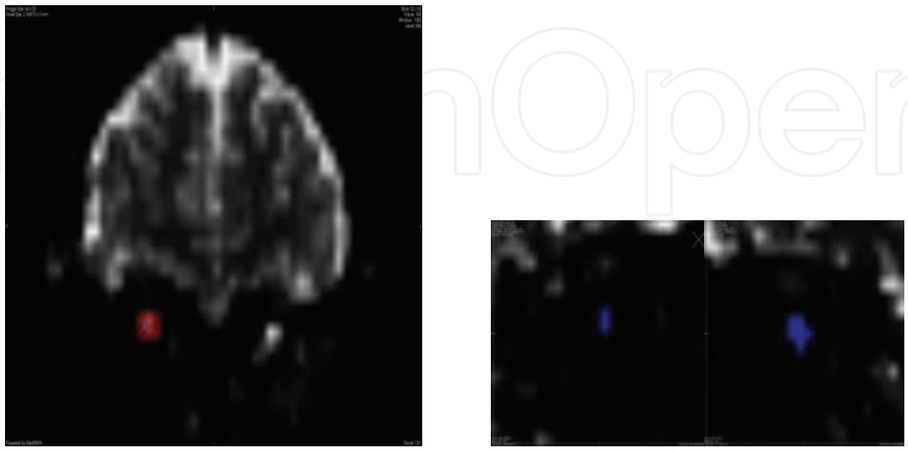

(A) (B)

Fig. 6. b0 coronal plane images of control (A) and AC with severe glaucoma in left eye (B).

In comparison with the control (Figure 7B) and opposite eye, a decrease in the thickness of the optic nerve on the severely glaucomatous side in the patient with asymmetrical involvement (Figure 7A) was clearly observed in optic nerve tractographies.

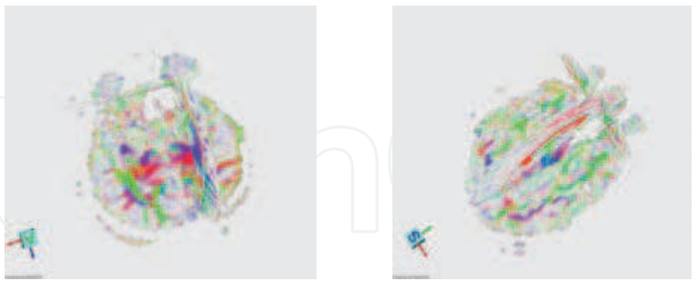

(A) (B)

Fig. 7. Color FA map optic nerve tractography of control (A) and AC with severe glaucoma in left eye (B).

In fMRI analyzes, data analyzes were performed with reference to VF obtained in subjects. BOLD signals obtained from each quadrant were recorded (Table 3). In the sensitive field analysis, success could not be gained since BOLD could not be obtained in all voxels.

	Upper Right		Upper Left		Lower Left		Lower Right	
	Left	Right	Left	Right	Left	Right	Left	Right
Control	2.68	2.34	2.81	2.44	2.8	2.57	2.75	2.4
AC	1.72*	1.25	1.26	1.73	1.31	1.76	1.29	1.75

Table 3. Recorded BOLD signals from each quadrant of the control and the patient with severe glaucoma in left eye. *Enhanced BOLD values in the severely effected eye.

In comparative analyzes on quadrants with VF defect, in the patient with asymmetrical involvement, BOLD values in the eye with heavier defect were lower than that of the other eye (Figures 8A and B).

3.4 Discussion

Glaucoma is a group of ocular diseases characterized with progressive optic nerve damage and loss of vision. Despite recent treatments efficiently reducing IOP, they reserve the above mentioned characteristics. This condition made neuro-protection a high-priority issue in glaucoma (Weinreb, 2007). However, studies focused on the glaucoma – brain relation, which have increased in number in recent years, have shown us that the posterior aspect of the retina and the head of the optic nerve should be considered when IOP-independent treatment is developed, and moreover, diffusion of neurodegeneration in the brain should be taken into consideration in the diagnosis and follow-up of glaucoma. More importantly, it is obvious that the damage is sustained (Yücel et al, 2003). Therefore, in this study, we aimed to create bulbar-retrobulbar, structural-functional integrity in the evaluation of glaucomatous neurodegeneration.

The DTI examination, the structural examination arm of our study, was performed in two stages. In DTI diffusion analyzes, the observation of reduction in all parameters in the severely glaucomatous eye in comparison with the other eye in the patient with

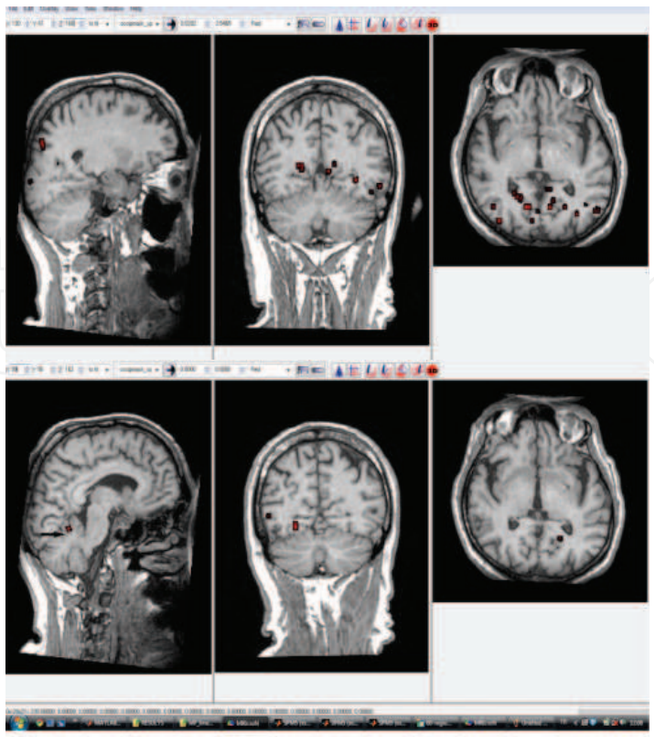

Fig. 8. For AC, BOLD signals of right eye inferior temporal quadrant (A) and left eye inferior temporal quadrant. Arrow: BOLD signal obtained in cerebellum due to movement of the patient

asymmetrical involvement is partially compatible with the literature. In the experimental glaucoma study conducted by Hui et al. on a mouse model, a decrease in FA values and an increase in λ1 values were observed in the optic nerve in glaucomatous eye and an increase in λ1 between Day 8 and Day 21 was found to be statistically significant (Hui et al, 2007). On the contrary, in the single study conducted on humans, an increase in MD values in addition to a decrease in FA values, which were parallel to findings of Hui et al., were reported (Garaci et al, 2009). Direct correlation of diffusion analyzes with findings of eye is not yet present in the literature.

Morphological findings obtained in the second stage of DTI outcomes are compatible with the literature. Degeneration in the glaucomatous optic nerve could be histologically demonstrated in mice (Hui et al, 2007), monkeys and humans (Gupta et al, 2006). Moreover, the degeneration could be demonstrated, as we imaged in humans using 1.5T and in the optic nerve on the coronal plane of small mice with 7T DTI, but it was reported as reduction rather than a temporal loss (Hui et al, 2007). Those findings match the above studies conducted on glaucoma patients with conventional MRI (Kashiwagi et al, 2004). On the contrary, lower volume in the control relative to the patient values can be explained on the basis that the diameter of optic nerve may have significant (in the range of 4-9 mm) inter-individual variation (Stark & Bradley, 1996).

In our study, functional evaluation was performed with VF and fMRI. However, it was observed that VF defects were also correlating with DTI findings. In fact, a defect in the visual field may originate from a pathology in any location ranging from the retina to the

cortex (Landers et al, 2004). It was reported that in normo-tensive glaucoma, deeper depressions were observed in the VF of the patient with ischemia in the brain MRI (Suzuki et al, 2004). In our study, in the comparative analysis of quadrants with VF defect, it was found that in the patient with asymmetrical involvement, BOLD values of the eye with serious defect were lower than that of the other eye.

The outstanding study of Duncan et al. (Duncan et al, 2007) is the only study in the literature where functional analysis with VF and MRI was conducted in glaucoma. In the study, the imaging of a defect of VF in the brain with 3T MRI using a long and complex stimulation was achieved. It is also possible to perform those precise analyzes using our multifocal mapping method; however, 3T MRI was used in the original method (Vanni et al, 2005). In the study, since BOLD could not be obtained in all voxels in sensitive area analysis with 1.5 T MRI, success could not be gained; however, an occipital cortex BOLD activity difference could be demonstrated in the highly asymmetrical patient.

In our study, an important aim, in our opinion, was to develop a method compatible with MRI devices routinely used in clinics, because we believe that large case series can only be obtained with this approach. Studies existing in the literature were performed with 3T MRI devices, which were generally used for experimental purposes, and with 6-7T MRI devices, which were solely used for experimental purposes. Moreover, there is no study in the literature which examines structural and functional ophthalmological diagnosis methods and DTI-MRI and fMRI techniques in combination.

In this pro-study, the glaucoma-brain connection has been demonstrated in humans. Visual pathways from the retina to the cerebral cortex have been evaluated both structurally and functionally with routine clinical instruments. Furthermore, results obtained were concordant with OCT and VF, in structural and functional analysis.

5. Conclusions

After many years of subsequent precious studies on glaucoma-brain connection, Gupta and Yucel conclude “Glaucoma as a neurodegenerative disease is a valid working hypothesis to understand neural injury in the visual system. Observations suggest that mechanisms independent of IOP are also implicated in glaucomatous degeneration. This paradigm may stimulate the discovery of innovative IOP-independent strategies to help prevent loss of vision in glaucoma patients”.

Strategies independent from IOP, concerning the area beyond the optic nerve head, are needed in the evaluation and treatment of glaucoma. Currently, it is possible to image visual pathways from the optic nerve to the cerebral cortex both structurally and functionally. As our pro-study showed, routine clinical instruments are also adequate for clinical trials to reveal the glaucoma-brain connection; however, more sophisticated techniques are being developed to illuminate that relation further. Better understanding of retrobulbar glaucomatous damage will enable us to determine more efficient diagnosis, follow-up and treatment strategies and facilitate the answering of some questions which remain unknown about this disease.

6. Acknowledgments

The author wish to thank to other members of “3B Study group” Bulent Yemişci MD (Bağcılar Education and Research Hospital, Dept Ophthalmology), Sibel Bayramoğlu MD,

Nurten Turan MD (Bakırköy ŞK Education and Research Hospital, Dept of Radiology), Cengizhan Öztürk MD PhD Prof, Onur Özyurt Msc, Esin Karahan Msc (Bosphorus University, Dept of Biomedical Engineering) for their ongoing efforts in imaging glaucomatous neurodegeneration, and to Gülgün Engin MD Prof (Istanbul University, Istanbul Faculty of Medicine, Dept of Radiology) for employing her drawing skills for the artwork in this chapter.

7. References

Boucard CC, Hoogduin JM, van der Grond J, Cornelissen FW. (2007). Occipital proton magnetic resonance spectroscopy (1H-MRS) reveals normal metabolite concentrations in retinal visual field defects. *PLoS ONE* 2(2): e222.

Chan KC, So KF, Wu EX. (2009). Proton magnetic resonance spectroscopy revealed choline reduction in the visual cortex in an experimental model of chronic glaucoma. *Exp Eye Res* 88(1):65-70.

Chidlow G, Wood JP, Casson RJ. (2007). Pharmacological neuroprotection for glaucoma. *Drugs* 67(5):725-759.

Duncan RO, Sample PA, Weinreb RN, Bowd C, Zangwill LM. (2007). Retinotopic organization of primary visual cortex in glaucoma: Comparing fMRI measurements of cortical function with visual field loss. *Prog Retin Eye Res* 26(1):38-56.

Engelhorn T, Michelson G, Waerntges S, Struffert T, Haider S, Doerfler A. (2011). Diffusion Tensor Imaging Detects Rarefaction of Optic Radiation in Glaucoma Patients. *Acad Radiol* Mar 4. [Epub ahead of print]

Garaci FG, Bolacchi F, Cerulli A, Melis M, Spanò A, Cedrone C, Floris R, Simonetti G, Nucci C. (2009). Optic nerve and optic radiation neurodegeneration in patients with glaucoma: in vivo analysis with 3-T diffusion-tensor MR imaging. *Radiology* 252(2):496-501.

Gupta N, Yücel YH. (2003). Brain changes in glaucoma. *Eur J Ophthalmol* 13 Suppl 3:S32-535.

Gupta N, Ang LC, de Tilly LN, Bidaisee L, Yucel YH. (2006). Human glaucoma and neural degeneration in intracranial optic nerve, LGN, and visual cortex. *Br J Ophthalmol* 90:674–678.

Gupta N, Yücel YH. (2007). Glaucoma as a neurodegenerative disease. *Curr Opin Ophthalmol* 18(2):110-114.

Hui ES, Fu QL, So KF, Wu EX. (2007). Diffusion tensor MR study of optic nerve degeneration in glaucoma. *Conf Proc IEEE Eng Med Biol Soc 2007* 2007:4312-4315.

Hood DC, Anderson SC, Wall M, Kardon RH. (2007). Structure versus function in glaucoma: an application of a linear model. *Invest Ophthalmol Vis Sci* 48:3662–3668.

Hood DC, Anderson SC, Wall M, Raza AS, Kardon RH. (2009). A Test of a Linear Model of Glaucomatous Structure–Function Loss Reveals Sources of Variability in Retinal Nerve Fiber and Visual Field Measurements *Invest Ophthalmol Vis Sci* 50:4254–4266

Kashiwagi K, Okubo T, Tsukahara S. (2004). Association of magnetic resonance imaging of anterior optic pathway with glaucomatous visual field damage and optic disc cupping. *J Glaucoma* 13(3):189-195.

Kitsos G, Zikou AK, Bagli E, Kosta P, Argyropoulou MI. (2009). Conventional MRI and magnetisation transfer imaging of the brain and optic pathway in primary open-angle glaucoma. *Br J Radiol* 82(983):896-900.

Knight OJ, Chang RT, Feuer WJ, Budenz DL. (2009). Comparison of retinal nerve fiber layer measurements using time domain and spectral domain optical coherent tomography. *Ophthalmology* 116(7): 1271–1277.

Landers J, Tang KC, Hing S. (2004). A visual field abnormality: ocular or cerebral cause? *Clin Experiment Ophthalmol* 32(2):219-222.

Lagrèze WA, Gaggl M, Weigel M, Schulte-Mönting J, Bühler A, Bach M, Munk RD, Bley TA. (2009). Retrobulbar optic nerve diameter measured by high-speed magnetic resonance imaging as a biomarker for axonal loss in glaucomatous optic atrophy. *Invest Ophthalmol Vis Sci* 50(9):4223-4228.

Lu K, Perthen JE, Duncan RO, Zangwill LM, Liu TT. (2008). Noninvasive measurement of the cerebral blood flow response in human lateral geniculate nucleus with arterial spin labeling fMRI. *Hum Brain Mapp* 29(10):1207-14.

Nucifora PGP, Verma R, Lee S, Melhem ER. (2007). Diffusion-Tensor MR Imaging and Tractography: Exploring Brain Microstructure and Connectivity. *Radiology* 245:367-384.

Qing G, Zhang S, Wang B, Wang N. (2010). Functional MRI signal changes in primary visual cortex corresponding to the central normal visual field of patients with primary open-angle glaucoma. *Invest Ophthalmol Vis Sci* 51(9):4627-4634.

Rauscher FM, Sekhon N, Feuer WJ, Budenz DL. (2009). Myopia affects retinal nerve fiber layer measurements as determined by optical coherence tomography. *J Glaucoma* 18(7): 501–505.

Sadun AA, Glaser JS, Bose S. (2007). Anatomy of the Visual Sensory System, In: *Duane's Ophthalmology*, Tasman W, Jaeger EA, (Eds.), Chapter 34, Lippincott Williams & Wilkins, ISBN 978-0-7817-6855-9, Philadelphia, PA, USA.

Sherbondy AJ, Dougherty RF, Napel S, Wandell BA. (2008). Identifying the human optic radiation using diffusion imaging and fiber tractography. *J Vis* 8(10):1-11.

Smith SM. (2002). Fast robust automated brain extraction. *Human Brain Mapping* 17(3):143-155

Stark DD, Bradley WG. (1996). Magnetic Resonance Imaging In: *Orbit*, Scott W. Pp 988-1028. Mosby, Missouri,USA.

Suzuki J, Tomidokoro A, Araie M, Tomita G, Yamagami J, Okubo T, Masumoto T. (2004). Visual field damage in normal-tension glaucoma patients with or without ischemic changes in cerebral magnetic resonance imaging. *Jpn J Ophthalmol* 48(4):340-344.

Vanni S, Henriksson L, James AC. (2005). Multifocal fMRI mapping of visual cortical areas. *Neuroimage* 27(1):95-105.

Weinreb RN. (2007). Glaucoma neuroprotection: What is it? Why is it needed? *Can J Ophthalmol* 42(3):396-398.

Yücel YH, Zhang Q, Weinreb RN, Kaufman PL, Gupta N. (2003). Effects of retinal ganglion cell loss on magno-, parvo-, koniocellular pathways in the LGN and visual cortex in glaucoma. *Prog Retin Eye Res* 22(4):465-481.

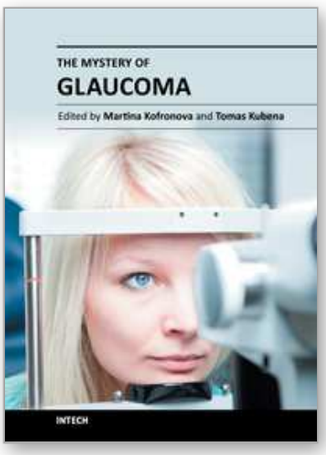

The Mystery of Glaucoma
Edited by Dr. Tomas Kubena

ISBN 978-953-307-567-9
Hard cover, 352 pages
Publisher InTech
Published online 06, September, 2011
Published in print edition September, 2011

Since long ago scientists have been trying hard to show up the core of glaucoma. To its understanding we needed to penetrate gradually to its molecular level. The newest pieces of knowledge about the molecular biology of glaucoma are presented in the first section. The second section deals with the clinical problems of glaucoma. Ophthalmologists and other medical staff may find here more important understandings for doing their work. What would our investigation be for, if not owing to the people's benefit? The third section is full of new perspectives on glaucoma. After all, everybody believes and relies – more or less – on bits of hopes of a better future. Just let us engage in the mystery of glaucoma, to learn how to cure it even to prevent suffering from it. Each information in this book is an item of great importance as a precious stone behind which genuine, through and honest piece of work should be observed.

INTECH
open science | open minds

InTech Europe
University Campus STeP Ri
Slavka Krautzeka 83/A
51000 Rijeka, Croatia
Phone: +385 (51) 770 447
Fax: +385 (51) 686 166
www.intechopen.com

InTech China
Unit 405, Office Block, Hotel Equatorial Shanghai
No.65, Yan An Road (West), Shanghai, 200040, China
中国上海市延安西路65号上海国际贵都大饭店办公楼405单元
Phone: +86-21-62489820
Fax: +86-21-62489821

IntechOpen